Proc. Nat. Acad. Sci. USA
Vol. 72, No. 1, pp. 51–55, January 1975

Crystal Structure of Human Erythrocyte Carbonic Anhydrase B. Three-Dimensional Structure at a Nominal 2.2-Å Resolution*

(x-ray diffraction/chain folding/active site/isoenzyme)

K. K. KANNAN, B. NOTSTRAND, K. FRIDBORG, S. LÖVGREN, A. OHLSSON, AND M. PETEF

The Wallenberg Laboratory, Uppsala University, Uppsala, Sweden

Communicated by John T. Edsall, October 7, 1974

ABSTRACT **The three-dimensional structure of carbonic anhydrase B (EC 4.2.1.1; carbonate hydro-lyase) from human erythrocytes has been determined to high resolution. Parallel and antiparallel pleated sheet makes up the predominant secondary structure of the enzyme. The tertiary structure is unique for its folding and is very similar to the structure of the isoenzyme, human erythrocyte carbonic anhydrase C. The essential metal ion, zinc, is firmly bound to the enzyme through three histidyl ligands and located at the bottom of a 12-Å deep conical cavity. The zinc ligands are involved in a number of hydrogen bond formations with residues in the immediate vicinity of the active site cavity. Some of the similarities and differences in the sidechain orientation and active site topography of the two isoenzymes are also discussed.**

Carbonic anhydrase (EC 4.2.1.1; carbonate hydro-lyase) is a zinc metalloenzyme and catalyzes the reversible reaction $CO_2 + H_2O \rightleftarrows HCO_3^- + H^+$ (1), the hydration of certain aldehydes (2), and the hydrolysis of certain esters (3, 4). The enzyme occurs in plants (5, 6), in certain bacteria (7), and in animals (8). In animals the enzyme is present in a great variety of cells and performs the fast hydration of metabolic CO_2 in the tissues and the dehydration of HCO_3^- in the lungs. Carbonic anhydrase is also involved in the transfer and accumulation of H^+ or HCO_3^- in organs of secretion (8). A recent review on carbonic anhydrase can be found in ref. 9.

Two major forms of carbonic anhydrase occur in human erythrocytes (10): the low activity form carbonic anhydrase B, and the high activity form carbonic anhydrase C. Carbonic anhydrase B is found in greater quantity than carbonic anhydrase C. The complete amino-acid sequences of the two isozymes have been established (11–14) and show a great deal of homology. The three-dimensional structure of carbonic anhydrase C has been established to 2-Å resolution (15, 16); the present article presents the high-resolution structure determination of carbonic anhydrase B.

MATERIALS AND METHODS

Crystallization and Heavy Atom Derivatives. Human carbonic anhydrase B was isolated from erythrocytes (kindly provided by the University Hospital, Uppsala) by mild methods (17). The enzyme was further purified by electrophoresis and on a Sulfur-ethylsephadex C-50 ion exchange column. Crystals of the native enzyme were prepared from 2.3 M ammonium sulfate, pH 8.7, by a seeding technique in small, thick-walled glass capillaries as described (18). Heavy atom derivatives were prepared by soaking native enzyme crystals for at least a week in 2.3 M ammonium sulfate solution, pH 8.7, containing 1 mM heavy atom salts, $K_2Au(CN)_2$, acetoxy mercury sulfanilamide, or acetazolamide. A fourth heavy atom derivative was prepared by removing the essential zinc ion with 2,3-dimercaptopropanol and replacing it with mercuric chloride as described (19).

Crystallography and Data Collection. Human carbonic anhydrase B crystallizes in the orthorhombic space group $P2_12_12_1$ with four molecules per unit cell of dimensions a = 81.5, b = 73.6, c = 37.1 Å (18, 20).

The diffraction data have been collected photographically with Burger-Supper precession cameras and Ni-filtered CuK α radiation. In general, one layer was collected per crystal and the total exposure time never exceeded 60 hr. The individual layers contained reflections with spacing greater than 2 Å. In all 30 layers, zero and upper levels were collected to cover about 85% of the reflections within the 2-Å sphere. Intensity measurements were performed by a fully automatic microdensitometer constructed by Ing. V. Klimecki of the Department of Chemistry, University of Uppsala, in collaboration with our group. The program system used for data processing was developed by one of us (K.K.K.) and is similar to that described by Järup *et al.* (21).

All the symmetry-related reflections were averaged, and the average amplitudes were used in subsequent calculations. The reflections in the 10-Å sphere and reflections below a threshold were omitted. Out of the 14,000 unique reflections thus measured, about 10,500 reflections were used in the refinements of heavy atom parameters, phase angle calculations, and electron density maps.

Heavy Atom Parameters and Phase Angle Calculation. The heavy atom positional parameters were initially determined from difference Patterson and difference Fourier calculations in two orthogonal projections. A single site mercury derivative (18) was used in the two centrosymmetric projections to calculate the signs used in the difference Fouriers from which the principal heavy atom positions were determined for the other derivatives. Subsequent cycles of least-squares refinement and difference Fouriers included all the derivatives. This procedure did not introduce any serious biasing effect due to the heavy atom derivatives concerned. Three-dimensional difference Patterson and correlation functions (22) were calculated to verify the correct assignment of the heavy atom positions. Alternate cycles of phase angle calculation and least-squares refinement were performed for relative scale factor, overall isotropic temperature factor, positional parameters, and anisotropic temperature factor for the heavy atoms of all the derivatives. The final parameters used in the phase angle calculations are shown in Table 1. The mean figure of merit was 0.68 for the 2500 reflections

* This is paper II in a series. Paper I is ref. 18.

TABLE 1. *Heavy atom parameters refined within a 2.0-Å sphere by the least-squares method*

Derivative	Site	Z	x	y	z	b_{11}	b_{22}	b_{33}	b_{12}	b_{23}	b_{13}	E	R_1	R_2
BAL + $HgCl_2$: Hg	H1	60	0.378	0.136	0.046	0.3	0.1	3.5	−0.1	−1.2	−0.3	35.3	0.09	0.39
	H2	34	0.452	0.227	0.399	0.2	0.01	0.6	0.6	−1.0	0.6			
$Au(CN)_2^-$: G	G1	45	0.405	0.196	0.509	0.8	0.3	4.2	0.03	0.9	1.9	36.2	0.11	0.59
	G2	14	0.060	0.124	0.891	1.1	0.4	7.0	0.9	2.5	−0.2			
Acetoxy mercury sulfanilamide: A	A1	58	0.379	0.135	0.041	0.6	0.6	5.2	−0.9	−1.9	0.1	40.4	0.11	0.55
	A2	19	0.357	0.100	0.055	0.2	0.001	3.0	−0.2	−0.2	1.0			
	A3	18	0.424	0.227	0.416	1.4	1.6	6.9	−1.6	4.7	−2.2			
	A4	16	0.423	0.215	0.506	1.0	4.4	16.9	3.2	−0.1	−0.8			
	A5	15	0.410	0.041	0.040	0.5	0.3	5.5	−0.6	−4.2	1.3			
Acetazolamide: X	X1	29	0.426	0.229	0.444	0.4	2.1	20.6	−0.2	1.5	0.5	39.3	0.11	0.75
	X2	21	0.413	0.208	0.515	3.3	5.5	0.9	7.7	0.8	0.9			
Zinc*		28	0.457	0.218	0.390									

$$R_1 = \frac{\Sigma\left||F_H| - ||F_p|\, e^{i\alpha} + f_c|\right|}{\Sigma|F_H|}; \quad R_2 = \frac{\Sigma\left||F_H - ||F_p|e^{i\alpha} + f_c|\right|}{\Sigma\left||F_H| - |F_p|\right|}$$

* Zinc coordinates were obtained from the electron density map. Z, occupancy of heavy atom site, electrons; b_{11}, b_{12} ...., anisotropic temperature factors × 10^3; E, averaged root mean square error from lack of closure refinement. BAL, 2,3-dimercaptopropanol. F_p, F_H, and f_c are structure factors for the native protein, the heavy atom derivative, and the calculated structure factors for the heavy atom contribution, respectively. α is the phase angle from the native enzyme.

with spacings smaller than 2.5 Å but larger than 2 Å. The average figure of merit for all the 10,500 reflections was 0.74.

A "best" Fourier synthesis (23) was calculated with 10,500 reflections and phase angles calculated from the parameters given in Table 1. Electron density maps were computed in sections perpendicular to the shortest unit cell direction, C, with an interval of 0.7 Å. The Fourier synthesis and the contouring was performed with a program kindly provided by Dr. G. N. Reeke in a scale of 2 cm to 1 Å. The lowest contour level was chosen at 0.45 e/Å^3, and subsequent contours were drawn at 0.25 e/Å^3. The printed contour outputs were traced on 75-μm Mylar sheets with the lowest contour level drawn in red and all other levels in black. The Mylar sheets were held in position by an inexpensive and space-saving rolling curtain device constructed in our workshop in collaboration with Dr. G. Söderlund, Chemistry Department, Agricultural College, Uppsala. The electron density maps were interpreted using Kendrew-Watson skeletal model parts in an optical comparator with the mirror mounted parallel to the plane of the maps (24, 25).

RESULTS

Interpretations. The molecular boundaries were easily located except where the neighboring molecules interact. The background density was generally low, and the polypeptide chain could be followed through most of the molecule. Occasional breaks in the otherwise continuous main chain density occurred usually on the surface of the molecule, e.g., the main chain density is poorly defined between residues 52 and 55.

Most of the carbonyl groups of the main chain were very well defined by the characteristic protrusion from the main chain density. Most of the forked residues were easily identified, and almost all the aromatic residues were recognizable by their well defined shape and density. Most of the proline residues were interpreted by their flat density appearing in the main chain density.

The model building was facilitated by the established chemical sequence available from different laboratories (11, 13, 14). The sequence of carbonic anhydrase, as determined by Nyman and coworkers (11), was found to give the best fit with the electron density maps.

The first four amino-acid residues have poorly defined density and were not built in the model. Otherwise, the number of residues built in the model (256) agrees very well with that established from sequence analysis (i.e., 256 + 4 = 260 amino acids). The prior knowledge of the sequence was found to be very helpful in the model building, and no special attempts were made to determine the sequence from the electron density maps. The chemical sequence of the isozyme carbonic anhydrase C is also available (12). To make meaningful comparisons with the three-dimensional structure of carbonic anhydrase C (15, 16), we have adopted the sequence numbering according to that of carbonic anhydrase B. Thus, residues 1 and 125 in carbonic anhydrase B are not present in carbonic anhydrase C, and 260 in carbonic anhydrase C is absent in carbonic anhydrase B.

Description of the Molecule. The carbonic anhydrase B molecule is approximately ellipsoidal, with dimensions 41 × 41 × 47 Å measured between extreme points of the backbone. The molecule can be likened to a sail boat, as seen in Fig. 1. The broad bottom is formed by residues 41–54, 150–170, 173–180, and 230 and the carboxyl terminal. The active site cavity is located on the deck, and the zinc ion is situated at the bottom of this cavity. Strands 120–138, 193–208, 240–250, and 20–40 form the cabin, and the amino-terminal residues 1–20 form the sail.

The active site is situated in a dead end cavity leading to the center of the molecule where the zinc ion is located. There are six pieces of right-handed helix, all located on the surface of the molecule on either side of a large β-structure formed by 10 polypeptide segments. There are a number of smaller β-structures located very near the surface of the molecule. There are also a number of reverse turns on either side of the large β-structure (26, 27).

Three distinct clusters involving aromatic residues almost equidistant from the zinc ion have been observed in carbonic anhydrase B. Fig. 1 is a schematic drawing of the main chain folding of carbonic anhydrase B. Fig. 2 is a stereoscopic

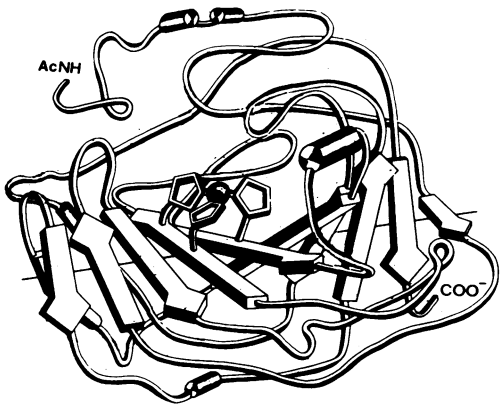

FIG. 1. A schematic drawing of the main chain of the carbonic anhydrase molecule. Cylinders represent helices and arrows represent β-structure. The dark ball in the middle is the essential zinc ion bonded to the protein by three histidyl ligands.

drawing of all the α-carbon atoms in carbonic anhydrase B except for the first four.

Secondary Structure. About 17% of all the residues are found in the seven helices. They are distributed on the surface of the molecule (Fig. 1). The helices are, in general, distorted and short. Only the helix formed by residues 217–223 is close to the α-helix conformation. All the others are close to the 3_{10} helical conformation, making about one helical turn each.

There are a number of hairpin-bends and type I and II reverse turns described by Venkatachalam (26) and Crawford *et al.* (27). These bends occur on the surface of the molecule. There are six reverse bends in carbonic anhydrase B, of which four are close to type I and 2 are type II bends. In two instances there are prolyl residues involved in these bends. Hydrogen bonds are not all formed in the plane of the peptide bonds.

The predominant secondary structure in carbonic anhydrase B is the pleated sheet, comprising about 40% of all the residues. The large twisted β-structure (Fig. 1), consisting of 10 chain segments, is a dominant characteristic of the carbonic anhydrase B molecule. There are two pairs of parallel chain segments in this β-structure, and the rest are antiparallel. The tenth chain segment is twisted from the first by about 220°. The main core of the molecule is formed by five chain segments, strands 2–6 in the β-structure, around which the rest of the polypeptide is wrapped. The active site cavity is also situated on these five chain segments, and the zinc ligands are located on chains 4 and 5 of the β-structure.

There are four smaller β-structures found in carbonic anhydrase B and located mainly on the surface of the molecule. These occur when the chain segments forming the large β-structure emerge on the surface and loop back into the interior region of the molecule to build up the large pleated sheet. The chain segments are all antiparallel in these small β-structures. The correlation between secondary structure expected from optical rotatory dispersion, circular dichroism, and infrared studies, on the one hand, and that observed from the x-ray structure, on the other, has been considered in the review article by Lindskog *et al.* (9) and is valid also for the carbonic anhydrase B structure.

Side Chain Location. The arrangement of side chains in carbonic anhydrase B follows the general principles of hydrophobic in and hydrophilic out. All the lysyl residues are on the surface of the molecule, as predicted by the amidination of all lysyl residues in carbonic anhydrase B (28). Except for two lysyl residues that interact with side chains in the neighboring molecules in the crystal structure, all the others are exposed to the solvent.

Three of 11 histidines are liganded to the metal ion and two are buried in the interior of the molecule. Of the remaining six histidines, three are located in the active site cavity and three are on the surface of the molecule. The two buried histidines interact with two buried tyrosine residues, as inferred by Riddiford *et al.* (29) from the titration data of histidines and tyrosines, that some of the tyrosines and histidines in carbonic anhydrase B would be buried in the molecule and are probably interacting with each other. Some of the tyrosines that are located on the surface interact with other side chain groups. Four tyrosyl residues of carbonic anhydrase B, 20, 88, 114, and 129, are located on the surface of the molecule. Three of the tryptophanyl residues are buried in the interior of the molecule, while two more are partially exposed to the solvent. Only Trp 4 is located on the surface of the molecule. One of the partially exposed tryptophans, Trp 122, is located in the entrance of the active site. Of the 11 phenyl-alanyl residues, eight are buried in the interior and are involved in the formation of the different aromatic clusters found in carbonic anhydrase B.

The only cysteinyl residue is not fully exposed to the solvent, but is accessible to small mercurials like $HgCl_2$. Both the methionyl residues in carbonic anhydrase B are located in the interior of the molecule and are inaccessible.

Prolyl residues are often exposed to the solvent and do not

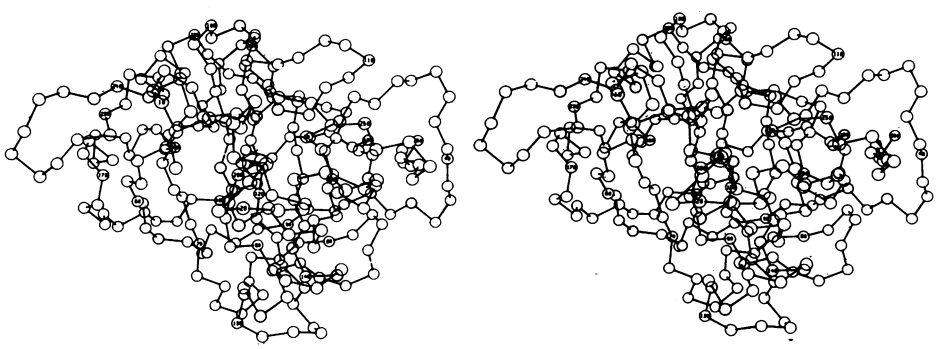

FIG. 2. Stereoscopic α-carbon diagrams of human carbonic anhydrase B. Dr. Carroll N. Johnson's ORTEP program was used to produce the computer drawings in this article.

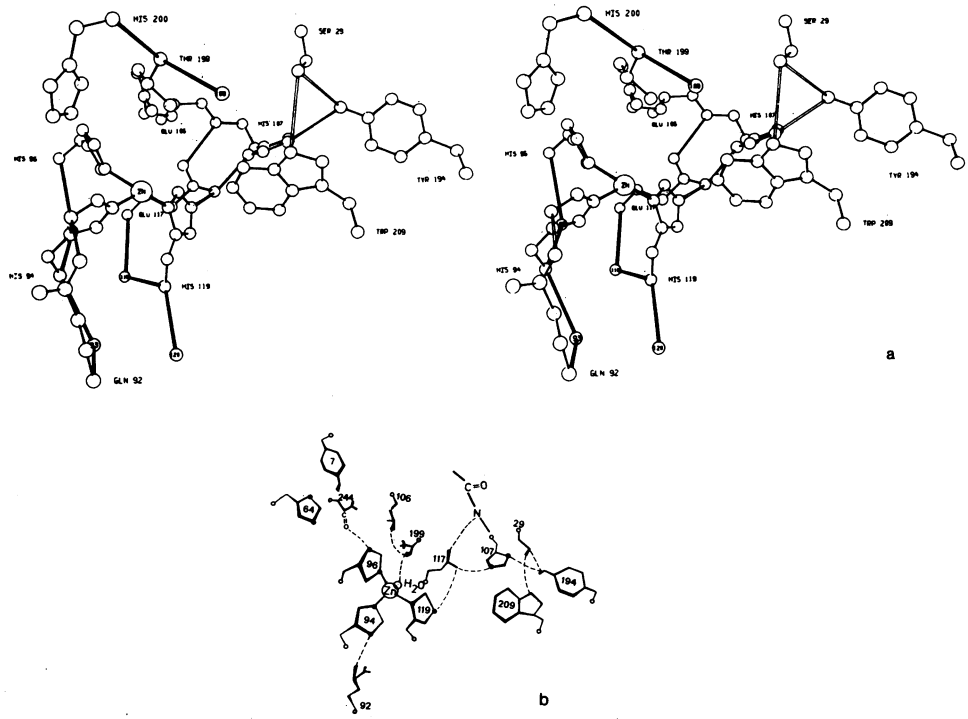

FIG. 3. a, Stereoscopic drawing of the hydrogen bond network of the active site. b, A schematic drawing of the hydrogen bonding observed in the active site.

seem to follow any general rules regarding their locations. There are 17 proline residues in carbonic anhydrase B. Two of these (Pro 30 and 202) could be fitted with the electron density only in the *cis* conformation and both occur as the third residue in an open reverse bend (27). *cis*-Prolines have been observed in other protein structures like ribonuclease (30) and subtilisin BPN′ (31).

The Active Site. The active site cavity is formed by portions of strands 3–6 of the big twisted β-structure. The rest of this large conical cavity is formed by two loops consisting of residues 121–138 and residues 198–204, and some of the residues in the amino terminus. The essential zinc ion is situated at the bottom of the cavity, about 12 Å from the entrance to the cavity. The metal is liganded to the protein by $N\epsilon_2$ of His 94 and 96 and $N\delta_1$ of His 119. A fourth ligand site is probably filled by a water molecule or OH ion, giving the zinc ion a distorted tetrahedral coordination (Fig. 3). His 94 is hydrogen bonded to Gln 92. His 119 is involved in a hydrogen bond network that involves several buried residues: Glu 117, His 107, Tyr 194, Ser 29, and Trp 209, as well as amide nitrogens N 106 and N 208 (Fig. 3a and b).

His 119 is hydrogen bonded to Glu 117, which is also hydrogen bonded to His 107 and to amide N 106. His 107 is hydrogen bonded to Tyr 194, which in turn is hydrogen bonded to Ser 29. Ser 29 is also hydrogen bonded to Trp 209 and amide N 208.

Zinc—His 119—Glu 117—His 107—Tyr 194—Ser 29—Trp 209
| |
N 106 N 208

It is not known at present if this hydrogen bond pattern has any functional significance or is formed for structural stabilization. The solvent molecule liganded to zinc is also hydrogen bonded to Thr 199, which is hydrogen bonded to a buried Glu 106.

The other striking feature of the active site cavity is the division into a hydrophobic half cone and a hydrophilic half cone. Serine 206 is located in the hydrophobic part of the cavity, which otherwise contains Ala 121 and 135, Val 207, Phe 91, Leu 131, 138, 146, and 109, and Pro 201 and 202. The hydrophilic part of the cavity consists of His 64, 67, and 200, Asn 69, and Gln 92. Thr 199, Tyr 7, and Val 62 are also located in this part of the cavity (Fig. 4).

The histidyl residues 67 and 200 have been modified by chlorothiazide (29) and bromoacetate (28, 32), respectively, with partial loss of activity. His 64, which is partially shielded by His 67 and His 200, has so far not been modified in carbonic anhydrase B.

Comparison Between the Structure of Carbonic Anhydrase B and Carbonic Anhydrase C. The knowledge of the molecular structures of the two isoenzymes and their respective sequences gives scope for some preliminary comparisons at the three-dimensional level.

The shape of the two molecules and the tertiary structure of the two enzymes are extremely similar [compare Fig. 2 with Fig. 5 of Kannan *et al.* (15)]. All the helices and β sheets and almost all the reverse bends are located homologously in the tertiary structure, even though the sequences are not entirely homologous in these regions.

The folding of carbonic anhydrases is different compared to those of other proteins whose three-dimensional structures are known.

In the carbonic anhydrase molecule the polypeptides are not folded in a number of sequential domains (33), as is the case with other proteins. Instead, the folding is achieved by a process of wrapping long segments of the polypeptide stabilized by β-structures and hydrophobic packing interactions. The only continuous domain-like feature in the carbonic anhydrases would be formed by residues 56–142, most of which are involved in strands 2–6 of the large β-structure.

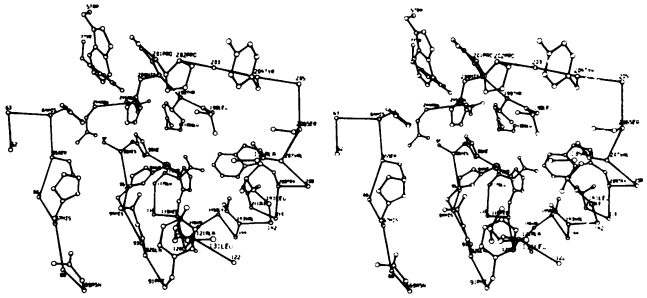

FIG. 4 The residues in the active site region.

The aromatic clusters are distributed in a similar fashion in the two enzymes and are formed by essentially homologous residues. Kannan *et al.* (15) have commented on the possible physicochemical significance of this type of arrangement.

The interactions between homologous histidines and tyrosines are observed in the two isozyme structures. The active sites of the isozymes are located on the strands 2–5 of the large β-structure. The active sites have similarly situated hydrophobic and hydrophilic halves. The essential zinc ion is liganded to homologous residues His 94, His 96, and His 119. The hydrogen bond arrangement involving His 119, Glu 117, His 107, Tyr 194, Ser 29, and Trp 209 is found in both the isozymes. The other invariant residues of the active site are Thr 199, Pro 201, and 202, His 64, and Gln 92.

There are also a number of differences in the two structures. Some of the important differences are observed in the active site cavity of the two enzymes. Thr 200 and Asn 67 in carbonic anhydrase C are replaced by histidines in carbonic anhydrase B. The topography of the active site in the immediate vicinity of zinc is different in the two enzymes due to these changes. Ile 91 in carbonic anhydrase C is replaced by Phe, and Phe 131 in carbonic anhydrase C by Leu, in carbonic anhydrase B. The hydrophobic part of the cavity in carbonic anhydrase C is more truly hydrophobic than that of carbonic anhydrase B. In this region the partially buried Cys in carbonic anhydrase C is replaced by Ser in carbonic anhydrase B, which is not, however, buried.

A more extensive comparison of the structures of carbonic anhydrase B and carbonic anhydrase C is presented elsewhere (34).

We thank Prof. B. Strandberg for fruitful discussions and support and encouragement throughout the work. We are very thankful to Drs. P. Lentz, A. Liljas, P. Nyman, and I. Vaara for stimulating discussions. We also thank Profs. C. Kurland and I. Olovsson for interest shown in this work and Prof. J. T. Edsall for valuable discussions. We are indebted to P. Krantz, C. Wallsten, and L. G. Petterson for constructing the optical comparator and to L. Lutter and G. Lindman for typing the manuscript, to H. Ukkonen for the photographic work, and to the staff of the Uppsala Data Center for helpful cooperation. This work was supported by grants from the Faculty of Science, University of Uppsala; the National Institutes of Health, U.S. Public Health Service (Grant no. AI 07382); the Swedish Computing Authorities; the Swedish Medical Science Research Council (Grant no. 13X-26); the Swedish Natural Science Research Council (Grant no. 2142); the Tricentennial Fund of the Bank of Sweden; and the Knut and Alice Wallenberg Foundation.

1. Meldrum, N. U. & Roughton, F. J. W. (1933) *J. Physiol.* **80**, 113–142.
2. Pocker, Y. & Meany, J. E. (1967) *Biochemistry* **6**, 239–246.
3. Schneider, F. & Liefländer, M. (1963) *Z. Physiol. Chem.* **334**, 279–282.
4. Tashian, R. E., Douglas, D. P. & Yu, Y. S. L. (1964) *Biochem. Biophys. Res. Commun.* **14**, 256–261.
5. Waygood, E. R. (1955) in *Methods in Enzymology*, eds. Colowick, S. P. & Kaplan, N. O. (Academic Press, New York), Vol. 2, pp. 836–846.
6. Tobin, A. J. (1970) *J. Biol. Chem.* **245**, 2656–2663.
7. Adler, L., Brundell, J., Falkbring, S. O. & Nyman, P. O. (1972) *Biochim. Biophys. Acta* **284**, 298–310.
8. Maren, T. H. (1967) *Physiol. Rev.* **47**, 595–781.
9. Lindskog, S., Henderson, L., Kannan, K. K., Liljas, A., Nyman, P. O. & Strandberg, B. (1971) in *The Enzymes*, ed. Boyer, P. D. (Academic Press, New York), 3rd ed., Vol. V, pp. 587–665.
10. Nyman, P. O. (1961) *Biochim. Biophys. Acta* **52**, 1–12.
11. Andersson, B., Nyman, P. O. & Strid, L. (1972) *Biophys. Res. Commun.* **48**, 670–677.
12. Hendersson, L. E., Henriksson, D. & Nyman, P. O. (1973) *Biochem. Biophys. Res. Commun.* **52**, 1388–1394.
13. Kuang-Tzu, D. L. & Deutsch, H. F. (1973) *J. Biol. Chem.* **248**, 1885–1893.
14. Foveau, D., Sciaky, M. & Laurent, G. (1974) *Biochimie* **278**, 959–962.
15. Kannan, K. K., Liljas, A., Waara, I., Bergstén, P.-C., Lövgren, S., Strandberg, B., Bengtsson, U., Carlbom, U., Fridborg, K., Järup, L. & Petef, M. (1971) *Cold Spring Harbor Symp. Quant. Biol.* **36**, 221–231.
16. Liljas, A., Kannan, K. K., Bergstén, P.-C., Waara, I., Fridborg, K., Strandberg, B., Carlbom, U., Järup, L., Lövgren, S. & Petef, M. (1972) *Nature New Biol.* **235**, 131–137.
17. Armstrong, J. M. D., Myers, D. V., Verpoorte, J. A. & Edsall, J. T. (1966) *J. Biol. Chem.* **241**, 5137–5149.
18. Kannan, K. K., Fridborg, K., Bergstén, P. C., Liljas, A., Lövgren, S., Petef, M., Strandberg, B., Waara, I., Adler, L., Falkbring, S. O., Göthe, P. O. & Nyman, P. O. (1972) *J. Mol. Biol.* **63**, 601–604.
19. Tilander, B., Strandberg, B. & Fridborg, K. (1965) *J. Mol. Biol.* **12**, 740–760.
20. Liljas, A., Kannan, K. K., Bergstén, P. C., Fridborg, K., Järup, L., Lövgren, S., Paradies, H., Strandberg, B. & Waara, I. (1969) in *CO_2: Chemical and Biochemical and Physiological Aspects*, eds. Forster, R. E., Edsall, J. T., Otis, A. B. & Roughton, F. J. W. (NASA, Washington D.C.), SP-188, pp. 89–99.
21. Järup, L., Kannan, K. K., Liljas, A. & Strandberg, B. (1970) *Comp. Progr. Biomed.* **1**, 74–76.
22. Kartha, G., Bello, J., Harker, D. & Dejernatte, F. E. (1963) in *Aspects of Protein Structure*, ed. Ramachandran, G. N. (Academic Press, London), pp. 13–22.
23. Blow, D. & Crick, F. H. C. (1959) *Acta Crystallogr.* **12**, 794–802.
24. Richards, F. M. (1968) *J. Mol. Biol.* **37**, 225–230.
25. Matthews, B. W., Jansonius, J. N., Colman, P. M., Schoenborn, B. P. & Dupourque, D. (1972) *Nature New Biol.* **238**, 37–41.
26. Venkatachalam, C. (1968) *Biopolymers* **6**, 1425–1436.
27. Crawford, J. L., Lipscomb, W. N. & Schellman, C. G. (1973) *Proc. Nat. Acad. Sci. USA* **70**, 538–542.
28. Whitney, P. L., Nyman, P. O. & Malmström, B. G. (1967) *J. Biol. Chem.* **242**, 4212–4220.
29. Riddiford, L. M. (1964) *J. Biol. Chem.* **239**, 1079–1086.
30. Wyckoff, H. W., Tsernoglou, D., Hanson, A. W., Knox, J. R., Lee, B. & Richards, F. M. (1970) *J. Biol. Chem.* **245**, 305–328.
31. Wright, C. S., Alden, R. A. & Kraut, J. (1969) *Nature* **221**, 235–242.
32. Whitney, P. L., Fölch, G., Nyman, P. O. & Malmström, B. G. (1967) *J. Biol. Chem.* **242**, 4206–4211.
33. Rossmann, M. G. & Liljas, A. (1974) *J. Mol. Biol.* **85**, 177–181.
34. Notstrand, B., Waara, I. & Kannan, K. K. (1974) in *The Proceedings of the Third International Conference on Isozymes*, ed. Markert, C. L. (Academic Press, New York.), in press.